Inorg. Chem. **2007**, *46*, 2452–2458

The Monolanthanide-Containing Silicotungstates $[Ln(\beta_2\text{-}SiW_{11}O_{39})_2]^{13-}$ (Ln = La, Ce, Sm, Eu, Gd, Tb, Yb, Lu): A Synthetic and Structural Investigation

Bassem S. Bassil, Michael H. Dickman, Bernd von der Kammer, and Ulrich Kortz*

School of Engineering and Science, International University Bremen,† P.O. Box 750 561, 28725 Bremen, Germany

Received September 13, 2006

We have synthesized and structurally characterized the monolanthanide-containing polyanions $[Ln(\beta_2\text{-}SiW_{11}O_{39})_2]^{13-}$ (Ln = La (**1**), Ce (**2**), Sm (**3**), Eu (**4**), Gd (**5**), Tb (**6**), Yb (**7**), Lu (**8**)). Synthesis was accomplished by reaction of the respective lanthanide ion with the monolacunary Keggin-type precursor $[\beta_2\text{-}SiW_{11}O_{39}]^{8-}$ in a 1:2 molar ratio in 1 M KCl medium at pH 5. Polyanions **1**–**8** were isolated as potassium salts and then characterized by IR, single-crystal X-ray diffraction, and elemental as well as thermogravimetric analysis. The structures of **1**–**8** are composed of an eight-coordinated Ln^{3+} center sandwiched by two chiral ($\beta_2\text{-}SiW_{11}O_{39}$) units. Large Ln^{3+} ions appear to favor an (*R*,*R*) (or (*S*,*S*)) configuration (point group C_2) of the Keggin units, with an increasing amount of (*R*,*S*) (or (*S*,*R*)) configuration (point group C_1) found in the solid state as the Ln^{3+} ion decreases in size. This trend is also supported by solution ^{183}W NMR results for the diamagnetic La^{3+} and Lu^{3+} derivatives.

Introduction

Polyoxometalates (POMs) have been known since the time of Berzelius, but it was not until a century later that Keggin reported the first POM structure.[1,2] POM chemistry has developed tremendously in the last 2−3 decades, mostly fueled by the discovery of many novel molecular structures with a large variety of sizes, shapes, and compositions. Furthermore, POMs are of major interest in many different areas, including catalysis, magnetism, nanotechnology, solid-state science, and medicine.[3]

Incorporation of transition metals into lacunary POM precursors can be considered as functionalizing the latter. Depending on the type and oxidation state of the transition metal, it may be possible to fine-tune the composition, size, shape, solubility, redox potentials, magnetic and catalytic properties, etc.[4] Also, lanthanide-containing POMs display many interesting properties, but to date, they have been much less investigated than first-row transition-metal-substituted polyanions. Due to their larger size, lanthanide ions have higher coordination numbers compared to those of the 3d metals. Thus, lanthanides are not fully inserted into the lacunary site(s) of vacant Keggin- or Wells−Dawson-type POM precursors. Each lanthanide ion has several (usually 2−4) additional coordination sites available, which can be used as linkers to one or more other lacunary POM units. This approach should, in theory, result in polymeric or unusually large molecular POM assemblies. The latter is beautifully demonstrated by Francesconi's tetrameric $[(PEu_2W_{10}O_{38})_4(W_3O_{14})]^{30-}$, by Gouzerh's $[Ce^{III}_3Sb_4W_2O_8(H_2O)_{10}(SbW_9O_{33})_4]^{19-}$, and, in particular, by Pope's cyclic $[As_{12}Ce_{16}(H_2O)_{36}W_{148}O_{524}]^{76-}$, the largest polyoxotungstate reported to date.[5−7] Interestingly, the last two polyanions could be synthesized without using any lacunary POM precursor.

Nevertheless, there are also reports on studies of lanthanide ions with monolacunary Keggin- and Wells−Dawson-type

* To whom correspondence should be addressed. E-mail: u.kortz@iu-bremen.de. Fax: +49-421-200 3229.

† Jacobs University Bremen as of Spring 2007.

(1) Berzelius, J. *Poggendorff's Ann. Phys.* **1826**, *6*, 369.

(2) (a) Keggin, J. F. *Nature* **1933**, *131*, 908. (b) Keggin, J. F. *Proc. R. Soc. London, Ser. A* **1934**, *144*, 75.

(3) (a) *Polyoxometalates: From Platonic Solids to Anti-Retroviral Activity*; Pope, M. T., Müller, A., Eds.; Kluwer: Dordrecht, The Netherlands, 1994. (b) *Chem. Rev.* **1998**, *98*, 1−389 (special thematic issue on polyoxometalates). (c) *Polyoxometalate Chemistry: From Topology via Self-Assembly to Applications*; Pope, M. T., Müller A., Eds.; Kluwer: Dordrecht, The Netherlands, 2001. (d) *Polyoxometalate Chemistry for Nano-Composite Design*; Yamase, T., Pope, M. T., Eds.; Kluwer: Dordrecht, The Netherlands, 2002.

(4) (a) Pope, M. T. *Compr. Coord. Chem. II* **2003**, *4*, 635. (b) Hill, C. L. *Compr. Coord. Chem. II* **2003**, *4*, 679. (c) *Polyoxometalate Molecular Science*; Borras-Almenar, J. J., Coronado, E., Muller, A., Pope, M. T., Eds.; Kluwer: Dordrecht, The Netherlands, 2004. (d) Casan-Pastor, N.; Gomez-Romero, P. *Front. Biosci.* **2004**, *9*, 1759.

10.1021/ic061737d CCC: $37.00
Published on Web 03/01/2007

POM precursors. In 1971, Peacock and Weakley reported the synthesis and elemental analysis of sandwich species with different lanthanides and monolacunary Keggin and Wells−Dawson units, but no structural characterization was provided.[8] Since then, several groups have studied this Weakley−Peacock species with the general formula $[LnL_2]^{n-}$, where Ln is a lanthanide ion and L is a monolacunary POM unit. In 1990, Fedotov et al. investigated the Keggin-based lanthanide derivatives $[Ln(PW_{11}O_{39})_2]^{11-}$ by multinuclear NMR.[9] Two Chinese groups reported crystal structures of the lanthanide-containing α-undecatungstosilicates $[Ln(\alpha\text{-}SiW_{11}O_{39})_2]^{13-}$ (Ln = Nd^{3+}, Pr^{3+}, Ce^{3+}).[10] In 1991, Qu et al. reported on the synthesis of several polyanions of the type $[Ln(\beta_2\text{-}SiW_{11}O_{39}]^{13-}$ (Ln = La, Ce, Pr, Nd, Sm, Gd, Er), but to date, no structural data supporting these results have been presented.[11] The Pope and Sécheresse groups reported chain-like, solid-state structures resulting from the interaction of lanthanide ions with the monolacunary silicotungstate $[\alpha\text{-}SiW_{11}O_{39}]^{8-}$.[12,13] Pope[14] and Francesconi[15] worked extensively on the interaction of lanthanides with the monolacunary Wells−Dawson ions $[x\text{-}A_2W_{17}O_{61}]^{10-}$ (A = P, As; $x = \alpha_1, \alpha_2$). In 2003, our group reported the novel La-containing, Wells−Dawson dimer $[\{La(CH_3COO)(H_2O)_2(\alpha_2\text{-}P_2W_{17}O_{61})\}_2]^{16-}$ with an acetate bridging the two La^{3+} ions.[16] In the following year, Mialane demonstrated the same acetate-bridging mode for the Keggin derivatives $[(\alpha\text{-}SiW_{11}O_{39}Ln)_2(\mu\text{-}CH_3COO)_2]^{12-}$ (Ln = Gd^{III}, Yb^{III}).[17] However, no structure of a lanthanide-containing polyanion based on the monolacunary, chiral Keggin precursor $[\beta_2\text{-}SiW_{11}O_{39}]^{8-}$ has been reported to date. The nonlacunary (plenary) α-Keggin ion is the most stable derivative and has ideal T_d symmetry. This polyanion is composed of four equivalent W_3O_{13} triads which consist of three edge-shared octahedra. These triads are connected to each other via corner-sharing of WO_6 octahedra. Rotating one of these triads by 60° results in the formation of the β-Keggin isomer with a symmetry reduced to C_{3v}. The monolacunary β_2-Keggin ion results from loss of one WO_6 octahedron adjacent to the rotated triad, resulting in C_1 symmetry (see Figure 1).

Experimental Section

Synthesis. The monolacunary Keggin precursor $K_8[\beta_2\text{-}SiW_{11}O_{39}]\cdot 14H_2O$ was synthesized according to the published procedure and identified in the solid state by FTIR.[18] All other reagents were used as purchased without further purification.

$K_{13}[La(\beta_2\text{-}SiW_{11}O_{39})_2]\cdot 22H_2O$ (K-1). To 20 mL of a 1 M KCl solution were added 0.032 g (0.085 mmol) of $LaCl_3\cdot 7H_2O$ and 0.500 g (0.155 mmol) of $K_8[\beta_2\text{-}SiW_{11}O_{39}]$. The pH of the solution was adjusted to 5.0 by dropwise addition of 0.1 M HCl. Then, the solution was stirred at 50 °C for 30 min and allowed to cool to room temperature. Filtration and slow evaporation in an open container at room temperature resulted in colorless crystals after about 1 week. Yield 0.45 g, 91%. IR data for **K-1** in cm^{-1}: 997 (m), 970 (m), 953 (m), 940 (m), 904 (s), 893 (s), 862 (s), 832 (m), 789 (s), 762 (sh), 722 (s), 530 (w). Anal. Calcd for **K-1**: K, 7.95; W, 63.3; La, 2.17; Si, 0.88. Found: K, 6.91; W, 65.1; La, 2.40; Si, 0.87. Tungsten-183 NMR of **K-1** in 2 M NaCl in H_2O/D_2O at 298 K: −89.4, −103.3, −105.4, −114.5, −136.3, −147.1, −164.5, −173.6, −178.5, −189.4, −196.7 ppm (all singlets).

$K_{13}[Ce(\beta_2\text{-}SiW_{11}O_{39})_2]\cdot 25.5H_2O$ (K-2). The same procedure as that for **K-1** was followed, except for using 0.032 g of $CeCl_3\cdot 7H_2O$. Yield 0.44 g, 88%. IR data for **K-2** in cm^{-1}: 998 (m), 969 (m), 952 (m), 939 (sh), 904 (s), 884 (s), 864 (s), 832 (m), 788 (s), 723 (s), 530 (w). Anal. Calcd for **K-2**: K, 7.9; W, 62.6; Ce, 2.2; Si, 0.9. Found: K, 7.9; W, 62.0; Ce, 2.4; Si, 1.0.

$K_{13}[Sm(\beta_2\text{-}SiW_{11}O_{39})_2]\cdot 29.5H_2O$ (K-3). The same procedure was followed using 0.031 g of $SmCl_3\cdot 6H_2O$. Yield 0.46 g, 91%. IR data for **K-3** in cm^{-1}: 1001 (m), 969 (m), 953 (m), 939 (sh), 908 (s), 886 (s), 867 (s), 835 (m), 793 (s), 762 (sh), 725 (s), 532 (w). Anal. Calcd for **K-3**: K, 7.8; W, 61.9; Sm, 2.3; Si, 0.9. Found: K, 7.4; W, 60.0; Sm, 1.8; Si, 1.1.

$K_{13}[Eu(\beta_2\text{-}SiW_{11}O_{39})_2]\cdot 25H_2O$ (K-4). The same procedure was followed using 0.031 g of $EuCl_3\cdot 6H_2O$. Yield 0.45 g, 90%. IR data for **K-4** in cm^{-1}: 1002 (m), 976 (m), 953 (m), 940 (m), 908 (s), 885 (s), 868 (s), 834 (s), 793 (s), 761 (sh), 721 (s), 530 (w), 469 (sh). Anal. Calcd for **K-4**: K, 7.9; W, 62.6; Eu, 2.4; Si, 0.9. Found: K, 7.8; W, 62.0; Eu, 2.0; Si, 1.0.

$K_{13}[Gd(\beta_2\text{-}SiW_{11}O_{39})_2]\cdot 27H_2O$ (K-5). The same procedure was followed using 0.032 g of $GdCl_3\cdot 6H_2O$. Yield 0.46 g, 91%. IR data for **K-5** in cm^{-1}: 1002 (m), 976 (sh), 953 (m), 941 (sh), 908 (s),

(5) Howell, R. C.; Perez, F. G.; Jain, S.; Horrocks, W. D., Jr.; Rheingold, A. L.; Francesconi, L. C. *Angew. Chem., Int. Ed.* **2001**, *40*, 4031.
(6) Xue, G. L.; Vaissermann, J.; Gouzerh, P. *J. Cluster Sci.* **2002**, *13*, 409.
(7) Wassermann, K.; Dickman, M. H.; Pope, M. T. *Angew. Chem., Int. Ed. Engl.* **1997**, *36*, 1445.
(8) (a) Peacock, R. D.; Weakley, T. J. R. *J. Chem. Soc. A* **1971**, 1836. (b) Peacock, R. D.; Weakley, T. J. R *J. Chem. Soc. A* **1971**, 1937.
(9) Fedotov, M.; Pertsikov, B.; Kanovich, D. *Polyhedron* **1990**, *9*, 1249.
(10) (a) Shan, Y.-K.; Liu, Z.-X. *Sci. China, Ser. B* **1991**, *34*, 313. (b) Shan, Y.-K.; Liu, Z.-X. *Acta Chim. Sin.* **1992**, 364. (c) Sun, R. Q.; Zhang, H. H.; Zhao, S. L.; Huang, C.-C.; Zheng, X. L. *Chin. J. Struct. Chem.* **2001**, *20*, 413.
(11) (a) Qu, L.; Niu, Z.; Liu, J.; Chen, Y.; Zhao, B.; Peng, J. *Gaodeng Xuexiao Huaxue Xuebao* **1991**, *12*, 1434. (b) Niu, Z.; Qu, L.; Chen, Y.; Peng, J.; Liu, J. *Yingyong Huaxue* **1992**, *9*, 46.
(12) Sadakane, M.; Dickman, M. H.; Pope, M. T *Angew. Chem., Int. Ed.* **2000**, *39*, 2914.
(13) Mialane, P.; Lisnard, L.; Mallard, A.; Marrot, J.; Antic-Fidancev, E.; Aschehoug, P.; Vivien, D.; Sécheresse, F. *Inorg. Chem.* **2003**, *42*, 2102.
(14) (a) Ostuni, A.; Bachman, R. E.; Pope, M. T. *J. Cluster Sci.* **2003**, *14*, 431. (b) Sadakane, M.; Ostuni, A.; Pope, M. T. *J. Chem. Soc., Dalton Trans.* **2002**, 63. (c) Ostuni, A.; Pope, M. T. *C. R. Acad. Sci., Ser. IIc: Chim.* **2000**, *3*, 199.
(15) (a) Boglio, C.; Lenoble, G.; Duhayon, C.; Hasenknopf, B.; Thouvenot, R.; Zhang, C.; Howell, R. C.; Burton-Pye, B. P.; Francesconi, L. C.; Lacote, E.; Thorimbert, S.; Malacria, M.; Afonso, C.; Tabet, J. C. *Inorg. Chem.* **2006**, *45*, 1389. (b) Zhang, C; Howell, R. C.; McGregor D.; Bensaid, L.; Rahyab, S.; Nayshtut, M.; Lekperic, S.; Francesconi, L. C. *C. R. Chim.* **2005**, *8*, 1035. (c) Zhang, C.; Howell, R. C.; Luo, Q. H.; Fieselmann, H. L.; Todaro, L. J.; Francesconi, L. C. *Inorg. Chem.* **2005**, *44*, 3569. (d) Zhang, C.; Howell, R. C.; Scotland, K. B.; Perez, F. G.; Todaro, L.; Francesconi, L. C. *Inorg. Chem.* **2004**, *43*, 7691. (e) Luo, Q. H.; Howell, R. C.; Bartis, J.; Dankova, M.; Horrocks, W. D., Jr.; Rheingold, A. L.; Francesconi, L. C. *Inorg. Chem.* **2002**, *41*, 6112. (f) Luo, Q. H.; Howell, R. C.; Dankova, M.; Bartis, J.; Williams, C. W.; Horrocks, W. D., Jr.; Young, V. G.; Rheingold, A. L.; Francesconi, L. C.; Antonio, M. R. *Inorg. Chem.* **2001**, *40*, 1894. (g) Bartis, J.; Dankova, M.; Lessmann, J. J.; Luo, Q. H.; Horrocks, W. D., Jr.; Francesconi, L. C. *Inorg. Chem.* **1999**, *38*, 1042. (h) Antonio, M. R.; Soderholm, L.; Jennings, G.; Francesconi, L. C.; Dankova, M.; Bartis, J. *J. Alloys Compd.* **1998**, *277*, 827. (i) Bartis, J.; Sukal, S.; Dankova, M.; Kraft, E.; Kronzon, R.; Blumenstein, M.; Francesconi, L. C. *J. Chem. Soc., Dalton Trans.* **1997**, 1937. (j) Bartis, J.; Dankova, M.; Blumenstein, M.; Francesconi, L. C. *J. Alloys Compd.* **1997**, *249*, 56.
(16) Kortz, U. *J. Cluster Sci.* **2003**, *14*, 205.
(17) Mialane, P.; Dolbecq, A.; Rivière, E.; Marrot, J.; Sécheresse, F. *Eur. J. Inorg. Chem.* **2004**, 33.
(18) (a) Tézé, A.; Hervé, G. *Inorg. Synth.* **1990**, *27*, 88. (b) Contant, R.; Tézé, A. *Inorg. Chem.* **1985**, *24*, 4610.

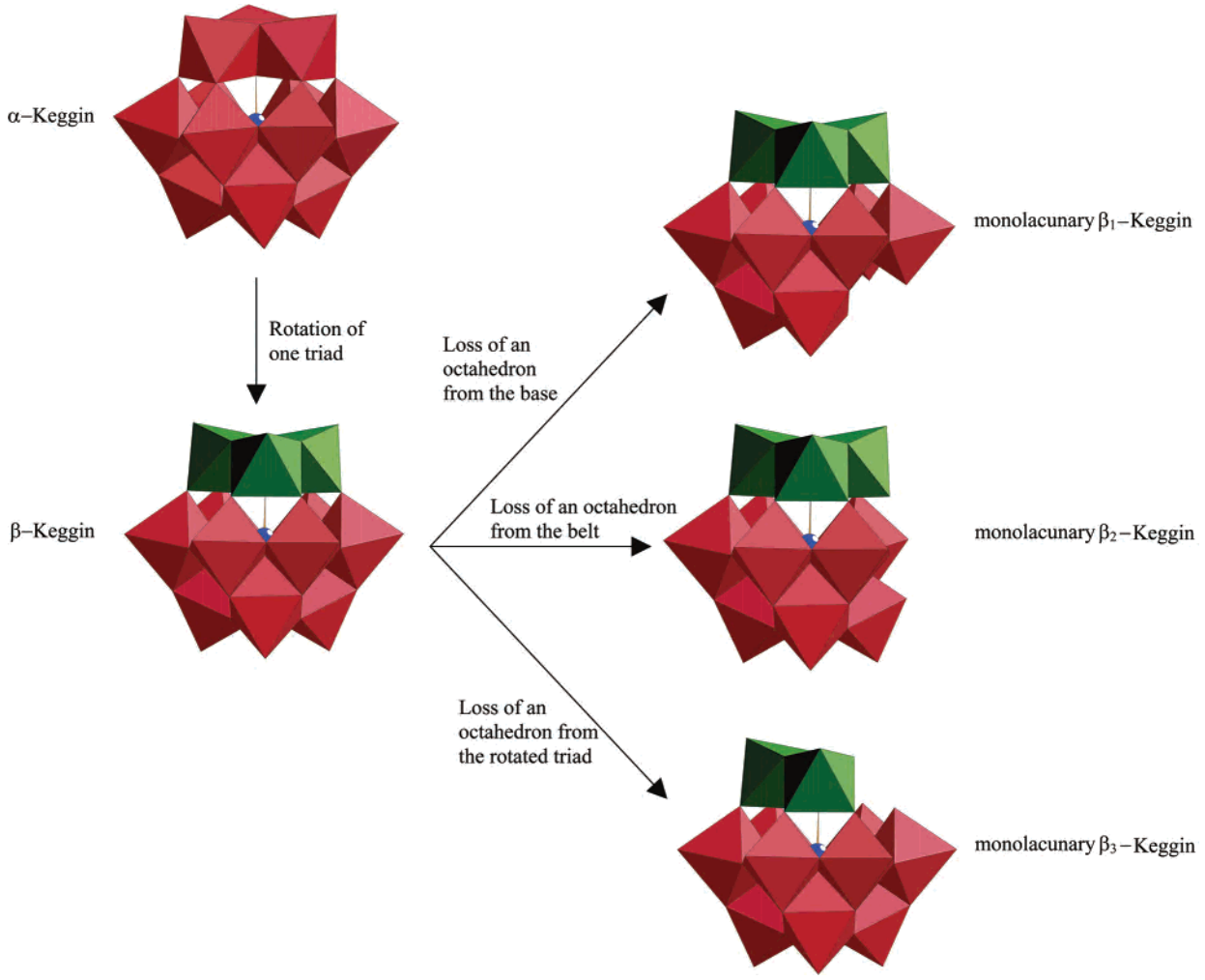

Figure 1. Structural relationship of the three monolacunary Keggin isomers $[\beta_1\text{-}SiW_{11}O_{39}]^{8-}$, $[\beta_2\text{-}SiW_{11}O_{39}]^{8-}$, and $[\beta_3\text{-}SiW_{11}O_{39}]^{8-}$ to the plenary derivatives $[x\text{-}SiW_{12}O_{40}]^{4-}$ ($x = \alpha, \beta$).

885 (s), 869 (s), 836 (m), 789 (s), 764 (sh), 723 (s), 530 (w), 467 (sh). Anal. Calcd for **K-5**: K, 7.82; W, 62.2; Gd, 2.42; Si, 0.86. Found: K, 7.38; W, 63.6; Gd, 2.40; Si, 0.93.

$K_{13}[Tb(\beta_2\text{-}SiW_{11}O_{39})_2]\cdot 29.5H_2O$ (K-6). The same procedure was followed using 0.030 g of $Tb(CH_3COO)_3\cdot H_2O$. Yield 0.44 g, 87%. IR data for **K-6** in cm^{-1}: 1006 (m), 969 (sh), 954 (m), 943 (sh), 910 (s), 886 (s), 869 (s), 836 (m), 793 (s), 764 (sh), 724 (s), 530 (w), 472 (sh). Anal. Calcd for **K-6**: K, 7.76; W, 61.8; Tb, 2.43; Si, 0.86. Found: K, 6.97; W, 62.9; Tb, 2.10; Si, 0.91.

$K_{13}[Yb(\beta_2\text{-}SiW_{11}O_{39})_2]\cdot 26H_2O$ (K-7). The same procedure was followed using 0.038 g of $Yb(NO_3)_3\cdot 5H_2O$. Yield 0.44 g, 87%. IR data for **K-7** in cm^{-1}: 1005 (m), 993 (sh), 957 (m), 906 (sh), 887 (s), 874 (sh), 838 (m), 791 (s), 724 (s), 532 (w), 477 (sh). Anal. Calcd for **K-7**: K, 7.82; W, 62.2; Yb, 2.66; Si, 0.86. Found: K, 7.22; W, 63.1; Yb, 2.30, Si, 0.93.

$K_{13}[Lu(\beta_2\text{-}SiW_{11}O_{39})_2]\cdot 27H_2O$ (K-8). The same procedure was followed using 0.031 g of $LuCl_3\cdot 6H_2O$. Yield 0.45 g, 89%. IR data for **K-8** in cm^{-1}: 1006 (m), 992 (sh), 956 (m), 906 (sh), 887 (s), 875 (sh), 839 (m), 791 (s), 768 (sh), 726 (s), 532 (w), 475 (sh). Anal. Calcd for **K-8**: K, 7.7; W, 61.5; Lu, 2.7; Si, 0.9. Found: K, 7.9; W, 59.0; Lu, 2.7; Si, 1.0.

Elemental analyses for **K-2**, **K-3**, **K-4**, and **K-8** were performed by ANALYTIS (Gesellschaft für Laboruntersuchungen mbH, 50389 Wesseling bei Köln, Germany), and elemental analyses for **K-1**, **K-5**, **K-6**, and **K-7** were performed by Analytische Laboratorien (Industriepark Kaiserau, 51789 Lindlar, Germany). Infrared spectra were recorded on KBr pellets using a Nicolet Avatar spectrophotometer. All NMR spectra were recorded on a 400 MHz JEOL ECX instrument at room temperature using H_2O/D_2O as the solvent. The ^{183}W NMR measurements were performed at 16.656 MHz in 10 mm tubes. Chemical shifts are reported with respect to 2 M Na_2WO_4, and the chemical shifts downfield of the reference are reported as positive. Thermogravimetric analyses were carried out on a TA Instruments SDT Q600 thermobalance with a 100 mL/min flow of nitrogen; the temperature was ramped from 20 to 800 °C at a rate of 2 °C/min.

X-ray Crystallography. Crystals were mounted in a Hampton cryoloop using light oil for data collection at low temperature. Indexing and data collection were performed using a Bruker X8 APEX II CCD diffractometer with kappa geometry and Mo Kα radiation ($\lambda = 0.71073$ Å). Data integration and routine processing were performed using the SAINT software suite. Further data processing, including absorption corrections from equivalent reflections, was performed using SADABS.[19] Direct methods (SHELXS97) solutions successfully located the W atoms, and successive Fourier syntheses (SHELXL97) revealed the remaining atoms.[20] Refinements were full-matrix least squares against F^2 using all data. Cations and waters of hydration were modeled with varying degrees of occupancy, a common situation for polyoxotungstate structures.

(19) Sheldrick, G. M. *SADABS*; University of Göttingen: Germany, 1996.
(20) Sheldrick, G. M. *SHELXS-97, Program for Solution of Crystal Structures*; University of Göttingen: Germany, 1997.

In the final refinements, all nondisordered heavy atoms (W, K, Si, Ln) were refined anisotropically, while the O atoms and some disordered cations were refined isotropically. No H atoms were included in the models. The crystallographic data are provided in Table 1.

Results and Discussion

Synthesis and Structure. Here, we report eight monolanthanide-containing, dimeric polyanions $[Ln(\beta_2\text{-}SiW_{11}O_{39})_2]^{13-}$ (Ln = La (**1**), Ce (**2**), Sm (**3**), Eu (**4**), Gd (**5**), Tb (**6**), Yb (**7**), Lu (**8**)). All derivatives **1**−**8** were prepared using the same synthetic procedure by reaction of the respective lanthanide ion with the monolacunary, chiral, Keggin-type precursor $[\beta_2\text{-}SiW_{11}O_{39}]^{8-}$ in a 1:2 molar ratio in 1 M KCl at pH 5. Polyanions **1**−**8** crystallize as hydrated potassium salts **K-1**−**K-8**. **K-1**−**K-6** crystallize in the monoclinic space group $P2_1/c$, whereas **K-7** and **K-8** are isostructural, and they crystallize in the orthorhombic space group *Pbca*.

Polyanions **1**−**8** are all composed of two chiral (β_2-$SiW_{11}O_{39}$) units sandwiching the Ln^{3+} ion, and at first sight, they all seem to have the same structure. However, close examination of the bonding situation around the central lanthanide ion in **1**−**8** reveals that bond lengths and angles, and especially the configurations of the two Keggin units, deserve special attention.

Polyanion **1** is composed of two (β_2-$SiW_{11}O_{39}$) units sandwiching a La^{3+} ion, which exhibits four La−O(W) bonds to each lacunary Keggin unit (see Figure 2). Rotation of the undecatungstosilicate fragments by about 40° with respect to each other results in an almost ideal square-antiprismatic coordination geometry for La^{3+}. It must be emphasized that **1** is composed of two chiral (β_2-$SiW_{11}O_{39}$) fragments such that the La^{3+} ion is situated in a vacancy of the Keggin unit which is adjacent to the rotated triad. As a result, the lanthanum center is coordinated to each monolacunary Keggin fragment via two oxygens of the incomplete triad, one oxygen of the rotated triad and one oxygen of the adjacent, nonrotated triad (see Figure 2). An alternative description is that the lanthanide center is coordinated to two oxygens from the belt, to one from the edge-shared (rotated) cap and to one from the corner-shared cap. The situation is similar for the Ce derivative **2**, which differs only by a slightly (∼1°) larger rotation angle between the two Keggin units compared to that of **1**.

Polyanions **3**−**6** have essentially the same molecular structure as **1** and **2**, but in the solid state, they exhibit two different configurations. This can be described as configurational disorder, where one of the two (β_2-$SiW_{11}O_{39}$) subunits has the position of the edge-shared and corner-shared triads exchanged through a mirror plane containing the silicon heteroatom and the five tungsten atoms of the belt (see Figure 3). We distinguish two configurations, the (*R*,*R*) or (*S*,*S*) configuration (A) and the (*R*,*S*) or (*S*,*R*) configuration (B), The symbols *R* and *S* define the relative chirality of each lacunary Keggin ion with respect to the other. The point group corresponding to configuration A is C_2, whereas it is C_1 for configuration B. For **3**, we observe

Table 1. Crystal Data and Structure Refinement for **K-1**−**K-8**

empirical formula	$K_{13}[La(SiW_{11}O_{39})_2]\cdot 22H_2O$ (**K-1**)	$K_{13}[Ce(SiW_{11}O_{39})_2]\cdot 25.5H_2O$ (**K-2**)	$K_{13}[Sm(SiW_{11}O_{39})_2]\cdot 29.5H_2$ (**K-3**)	$K_{13}[Eu(SiW_{11}O_{39})_2]\cdot 25H_2O$ (**K-4**)	$K_{13}[Gd(SiW_{11}O_{39})_2]\cdot 27H_2O$ (**K-5**)	$K_{13}[Tb(SiW_{11}O_{39})_2]\cdot 29.5H_2O$ (**K-6**)	$K_{13}[Yb(SiW_{11}O_{39})_2]\cdot 26H_2O$ (**K-7**)	$K_{13}[Lu(SiW_{11}O_{39})_2]\cdot 27H_2O$ (**K-8**)
MW	6392.5	6456.8	6539.1	6459.7	6501.0	6547.7	6498.7	6518.7
crystal system	monoclinic	monoclinic	monoclinic	monoclinic	monoclinic	monoclinic	orthorhombic	orthorhombic
space group (no.)	$P2_1/c$ (14)	$P2_1/c$ (14)	$P2_1/c$ (14)	$P2_1/c$ (14)	$P2_1/c$ (14)	$P2_1/c$ (14)	*Pbca* (61)	*Pbca* (61)
a/Å	18.7300(13)	18.6232(13)	18.7442(5)	18.7596(5)	18.7494(10)	18.7191(6)	21.3738(5)	25.3783(9)
b/Å	20.0384(11)	19.9618(12)	20.0470(5)	20.0516(5)	20.0610(9)	20.0259(5)	38.3275(10)	21.3325(6)
c/Å	27.5289(19)	27.4783(13)	27.3945(5)	27.3865(5)	27.3796(14)	27.3498(6)	25.3172(7)	38.3131(14)
α/°	90	90	90	90	90	90	90	90
β/°	96.966(4)	97.120(3)	97.439(1)	97.536(1)	97.586(3)	97.612(1)	90	90
γ/°	90	90	90	90	90	90	90	90
V/Å^3	10255.9(12)	10136.4(10)	10207.3(4)	10212.7(4)	10208.2(9)	10162.2(6)	20740.0(9)	20742.0(12)
Z	4	4	4	4	4	4	8	8
T/°C	−100	−100	−100	−100	−100	−100	−110	−100
λ/Å	0.71073	0.71073	0.71073	0.71073	0.71073	0.71073	0.71073	0.71073
D_c/Mg m^{-3}	3.956	3.962	3.923	3.980	3.957	3.939	4.065	4.029
μ/mm^{-1}	25.458	25.761	25.700	25.722	25.785	25.902	25.738	25.725
$R[I < 2\sigma(I)]^a$	0.063	0.068	0.085	0.068	0.088	0.073	0.064	0.060
R_w (all data)^b	0.197	0.222	0.270	0.202	0.285	0.221	0.175	0.173

^{a} $R = \sum||F_o| - |F_c||/\sum|F_o|$. ^{b} $R_w = [\sum w(F_o^2 - F_c^2)^2/\sum w(F_o^2)^2]^{1/2}$.

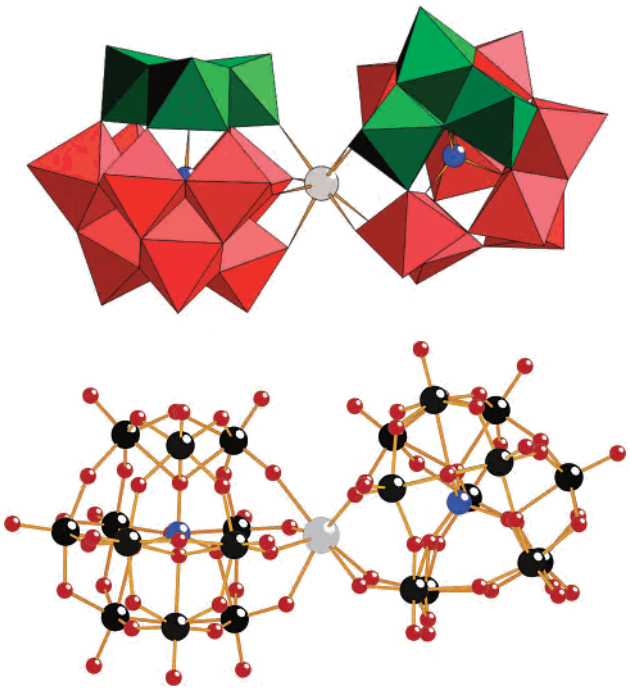

Figure 2. Polyhedral (upper) and ball-and-stick (lower) representation of $[La(\beta_2\text{-}SiW_{11}O_{39})_2]^{13-}$ (**1**). The color code is as follows: tungsten (black); oxygen (red); silicon (blue); La (gray). This structure is also representative for the other lanthanide derivatives $[Ln(\beta_2\text{-}SiW_{11}O_{39})_2]^{13-}$ (Ln = Ce (**2**), Sm (**3**), Eu (**4**), Gd (**5**), Tb (**6**), Yb (**7**), Lu (**8**)), but they exhibit slightly different degrees of rotation of the two Keggin fragments with respect to each other (see text for details). In the polyhedral presentation, the rotated triad was colored green for clarification.

an A/B crystallographic disorder of 60:40%, and for **4**−**6**, we observe essentially statistical (50:50%) A/B disorder. Here, the positions of the oxygens bridging to the Ln^{3+} ion are not disordered, and as a result, the local coordination environment of the lanthanide center is not affected.

Polyanions **1** and **2** both exhibit configuration A as 100% in the crystal studied, whereas polyanions **7** and **8** both exhibit configuration B as 100% in the crystal studied. Our results lead us to the conclusion that, in $[Ln(\beta_2\text{-}SiW_{11}O_{39})_2]^{13-}$, the size of the lanthanide ion determines which configuration is favored. For early (large) lanthanide ions like La^{3+} and Ce^{3+}, configuration A is strongly favored, whereas for the lanthanide ions in the middle of the 4f period, there is a gradual transition from configuration A to configuration B. Finally, the late (small) lanthanide ions Yb^{3+} and Lu^{3+} strongly favor configuration B.

We can also quantify the above observation by using the twist angle θ, which measures the relative orientation of the two rotated triads (one on each Keggin unit). Also, θ refers to the offset of the two squares built up from the respective four oxygens (O_u, O_t, $O1_e$, $O2_e$ and O_u', O_t', $O1_e'$, $O2_e'$) at the lacunary site of each of the two Keggin units (see Figure 4). More precisely, θ describes the rotation angle between the two planes formed by the following three atoms of each Keggin unit: the lanthanide center, its coordinated oxygen atom of the rotated triad (edge-shared cap), and the coordinated oxygen of the corner-shared cap. Francesconi et al. used the same method but different atoms to calculate the offset of the two Keggin halves for their studies on $[Ln(\alpha\text{-}SiW_{11}O_{39})_2]^{13-}$.[15i] Figure 3 shows the respective twist angle(s) θ for **1**−**8** in the solid state.

Polyanion **7** shows an additional, subtle type of disorder in the solid state, which is best described as $\beta-\alpha$ isomerization. In the crystal of **K-7** studied, a small fraction of the dimeric polyanion **7** actually contained an ($\alpha\text{-}SiW_{11}O_{39}$) unit, that is, a monolacunary Keggin fragment with no rotated triad. Only one of the two ($SiW_{11}O_{39}$) units in **7** exhibits this phenomenon and only to a very small degree. We were able to model this disorder satisfactorily by assigning partial occupancies of 0.9/0.1 to the six tungsten centers in question, and therefore, the α isomerization was found to account for only about 10% of the overall structure. This observation suggests partial transformation of the all-β isomer **7** to the (most likely more stable) all-α isomer $[Yb(\alpha\text{-}SiW_{11}O_{39})_2]^{13-}$ in solution. It is very likely that this transformation proceeds via the $\alpha\text{-}\beta_2$-intermediate $[Yb(\alpha\text{-}SiW_{11}O_{39})(\beta_2\text{-}SiW_{11}O_{39})]^{13-}$. This reflects the well-known solution transformation pattern of the monolacunary silicotungstate Keggin precursors, $[\beta_2\text{-}SiW_{11}O_{39}]^{8-} \rightarrow [\beta_3\text{-}SiW_{11}O_{39}]^{8-} \rightarrow [\alpha\text{-}SiW_{11}O_{39}]^{8-}$, as shown by Tézé and Hervé.[18] These observations are also fully consistent with our solution NMR studies on **K-1** and **K-8** (*vide infra*).

In order to verify the expected decrease of the Ln−O bond lengths with increasing atomic number of Ln, we determined average Ln−O bond lengths for **1**−**8**. The results (see Table 2) show the expected trend, which reflects the decreasing size from early to late Ln^{3+} ions.

We also performed ^{183}W NMR studies on the diamagnetic polyanions **1** and **8** in order to learn more about the solution behavior of these species. Francesconi and co-workers have studied the all-α derivatives of **1** and **8** by ^{183}W NMR.[15i] For our measurements, we redissolved the maximum amount of solid **K-1** and **K-8** in H_2O/D_2O. For **K-1**, we discovered that, after an overnight ^{183}W measurement at room temperature, the 6-line spectrum was identical to that reported by Francesconi et al. for the all-α isomer $[La(\alpha\text{-}SiW_{11}O_{39})_2]^{13-}$.[15i] In a second experiment using identical conditions, we monitored the evolution of the ^{183}W spectrum with time. We discovered that, already, the first peaks visible after a few hours correspond to Francesconi's $[La(\alpha\text{-}SiW_{11}O_{39})_2]^{13-}$. Then, we searched for a different solvent medium which could, perhaps, stabilize **1** better than pure water, and we identified a 2 M NaCl, pH 5.5 solution as an appropriate choice. A room-temperature, overnight ^{183}W measurement on **K-1** redissolved in 2 M NaCl (pH 5.5) resulted in a spectrum with 11 peaks of about equal intensity (−89.4, −103.3, −105.4, −114.5, −136.3, −147.1, −164.5, −173.6, −178.5, −189.4, and −196.7 ppm, see Figure 5). This spectrum reflects the C_2 symmetry of **1** in the solid state (see Figure 1). Careful inspection of the spectrum reveals five additional peaks of lower intensity (−91.9, −136.8, −143.0, −166.3, and −200.0 ppm, see Figure 5), which we assign to the all-α isomer $[La(\alpha\text{-}SiW_{11}O_{39})_2]^{13-}$. One more peak is expected for this isomer, but it is most likely obscured by one of the other 11 peaks of **1**. Partial transformation of **1** to the all-α isomer during the overnight measurement is not unexpected. In fact, increased heating resulted in a

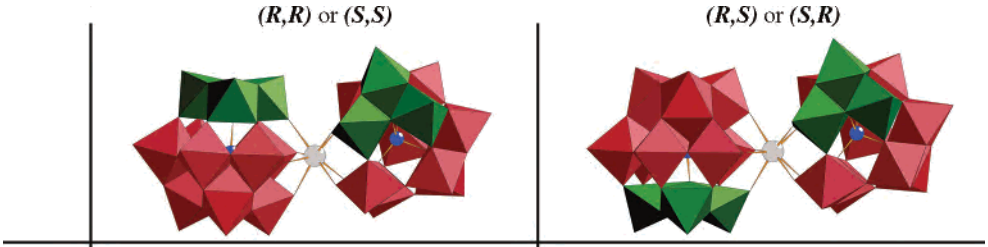

	Configuration percentage	θ (esd)	Configuration percentage	θ (esd)
La	100%	39.9 (6)		
Ce	100%	40.8 (8)		
Sm	60%	41.3 (9)	40%	-138.7 (9)
Eu	50%	44.4 (8)	50%	-135.6 (8)
Gd	50%	42.9 (8)	50%	-137.1 (8)
Tb	50%	44.6 (6)	50%	-135.4 (6)
Yb			100%	-131.7 (7)
Lu			100%	-132.4 (7)

Figure 3. The two possible configuration isomers of **1**−**8** are shown along with the respective percentages for each with the corresponding twist angle θ. For clarity, the right Keggin subunit was left unchanged in both representations. The color coding is the same as in Figure 2.

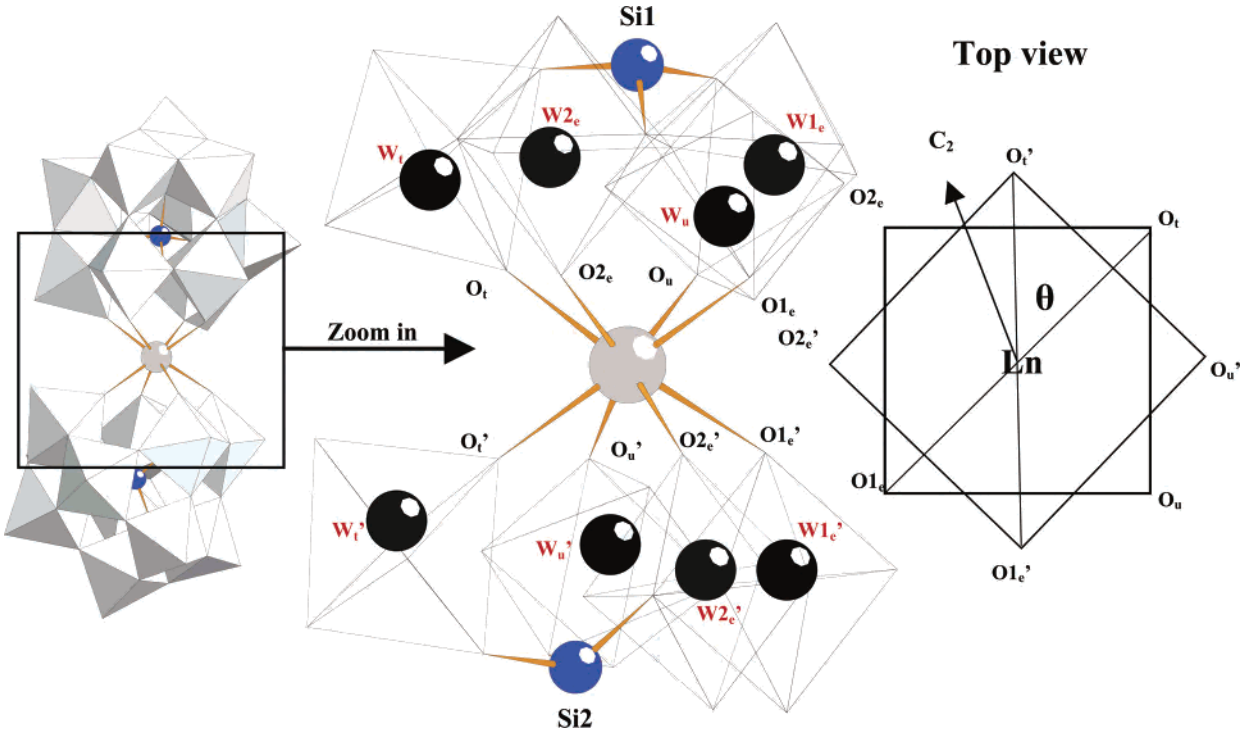

Figure 4. This figure highlights the inner coordination sphere of the lanthanide centers in **1**−**8**. It also shows how the twist angle θ is determined. The subscript e indicates that this oxygen belongs to an edge-sharing octahedron, the subscript u indicates that this oxygen belongs to an unshared octahedron, and the subscript t indicates that this oxygen belongs to an octahedron of the rotated triad. The two-fold rotation axis of **1** and **2** is also shown.

Table 2. Average Ln−O Bond Lengths in $[Ln(\beta_2\text{-}SiW_{11}O_{39})_2]^{13-}$ (Ln = La (**1**), Ce (**2**), Sm (**3**), Eu (**4**), Gd (**5**), Tb (**6**), Yb (**7**), Lu (**8**))

Ln	average Ln−O(W) bond lengths in Å
La (**1**)	2.49(3)
Ce (**2**)	2.46(2)
Sm (**3**)	2.41(3)
Eu (**4**)	2.40(3)
Gd (**5**)	2.40(3)
Tb (**6**)	2.37(3)
Yb (**7**)	2.33(3)
Lu (**8**)	2.321(15)

significantly faster transformation of **1** to $[La(\alpha\text{-}SiW_{11}O_{39})_2]^{13-}$, accompanied by an increase of the 5 peaks and a decrease of the 11 peaks due to **1**. We conclude that the all-α isomer $[La(\alpha\text{-}SiW_{11}O_{39})_2]^{13-}$ is thermodynamically more stable than the β_2-isomer **1**. This is also in agreement with the work of Tézé and Hervé who concluded that $[\beta_2\text{-}SiW_{11}O_{39}]^{8-}$ is less stable than $[\alpha\text{-}SiW_{11}O_{39}]^{8-}$.[18] As indicated above, these authors showed that, in aqueous solution, $[\beta_2\text{-}SiW_{11}O_{39}]^{8-}$ transforms to $[\alpha\text{-}SiW_{11}O_{39}]^{8-}$ via the $[\beta_3\text{-}SiW_{11}O_{39}]^{8-}$ intermediate. We speculate that the transformation of $[Ln(\beta_2\text{-}SiW_{11}O_{39})_2]^{13-}$ to the corresponding all-α isomer proceeds via the Tézé−Hervé mechanism by initial dissociation of one lacunary Keggin unit followed by rearrangement to its α-isomer and recoordination to the $[Ln(\beta_2\text{-}SiW_{11}O_{39})]^{5-}$ fragment. This is consistent with our observation that high

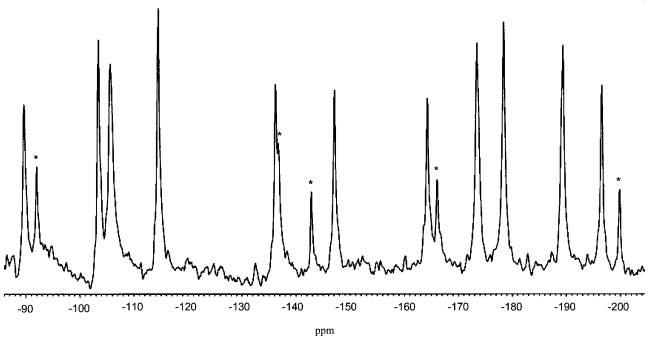

Figure 5. Tungsten-183 NMR spectrum of $K_{13}[La(\beta_2\text{-}SiW_{11}O_{39})_2]\cdot 22H_2O$ (**K-1**) in 2M NaCl (pH 5.5) at 293 K. The peaks with an asterisk most likely represent the all-α isomer $[La(\alpha\text{-}SiW_{11}O_{39})_2]^{13-}$ due to partial transformation of **1** (see text for details).

concentrations of alkali metal ions slow down the isomerization pathway (β_2-$SiW_{11}O_{39}$) → (β_3-$SiW_{11}O_{39}$) → (α-$SiW_{11}O_{39}$) likely by occupying the lacunary site of the dissociated $[\beta_2\text{-}SiW_{11}O_{39}]^{8-}$ fragment.

The ^{183}W NMR studies on the Lu-derivative **K-8** in 2 M NaCl (pH 5.5) revealed around 22 peaks between −81.8 and −230.3 ppm. This is fully consistent with the observed C_1 symmetry of **8** in the solid state.

Furthermore, we performed thermogravimetric analyses (TGA) on all eight compounds **K-1**−**K-8** under a N_2 atmosphere. These measurements allowed us to evaluate the thermal stability of polyanions **1**−**8** in the solid state (see Figures S1−S8). By using this technique, we could also determine the number of water molecules of hydration. As expected, the thermograms of **K-1**−**K-8** all look fairly similar. The compounds **K-1**−**K-8** start to lose crystal water almost instantaneously upon heating from room temperature up to around 200 °C, after which there is no weight loss for **K-1**−**K-7** up to the final temperature at 800 °C. Only the lutetium derivative **K-8** exhibits a second weight-loss step at around 530 °C. Our TGA studies indicate that **K-1**−**K-7** dehydrate completely and are thermally stable up to 800 °C. The degrees of hydration for **K-1**−**K-8** range from 22 to 29.5 water molecules.

Conclusions

The solution and solid-state chemistry and reactivity of silicotungstates is well developed, but the monolacunary $[\beta_2\text{-}SiW_{11}O_{39}]^{8-}$ Keggin precursor has been pretty much neglected. This is interesting, as this species represents a rare example of a lacunary POM which is chiral. One reason for the lack of using $[\beta_2\text{-}SiW_{11}O_{39}]^{8-}$ as a precursor reagent is probably due to the fact that it is rather unstable, transforming easily to the β_3- and α-derivatives in aqueous solution. In other words, it is difficult to preserve the β_2-Keggin framework in the final polyanion products. Our work has shown that reaction with lanthanide ions allows the (β_2-$SiW_{11}O_{39}$) fragment to be stabilized in the form of the dimeric assembly $[Ln(\beta_2\text{-}SiW_{11}O_{39})_2]^{13-}$ (Ln = La (**1**), Ce (**2**), Sm (**3**), Eu (**4**), Gd (**5**), Tb (**6**), Yb (**7**), Lu (**8**)). To our knowledge, these are the first examples of structurally characterized POM derivatives based on $[\beta_2\text{-}SiW_{11}O_{39}]^{8-}$ as the precursor and constituent building block. We have obtained a total of eight polyanion structures, including early, middle, and late lanthanides. This number of derivatives allowed us to carefully evaluate the bonding situation (lengths, angles) around the lanthanide center and, most importantly, the relative orientation of the chiral Keggin units with respect to each other as a function of the size of the lanthanide center. We discovered a pattern showing that one configuration is favored for early lanthanides and the other for late lanthanides, with a gradual transition from one to the other throughout the lanthanide series. This phenomenon resulted in what we describe as configurational disorder in the solid-state X-ray structures. Last, we also performed solution ^{183}W NMR studies on the two diamagnetic La and Lu derivatives **1** and **8**, and the spectra are consistent with the POM symmetries observed in the solid-state structures. Moreover, we discovered that the solvent medium plays an important role in the stabilization of **1**−**8**. A high concentration of alkali-metal ions seems to prolong the lifetime of the β-Keggin isomer, as observed by ^{183}W NMR. In conclusion, our work shows that unstable, lacunary polyanion fragments can be stabilized by lanthanide centers in solution and in the solid state.

Acknowledgment. This work was supported by the International University Bremen. Figures 1 and 2 were generated by Diamond Version 3.1a (copyright, Crystal Impact GbR). We thank Alexandra Dumitriu for help in the laboratory.

Supporting Information Available: X-ray crystallographic files in CIF format and thermograms for **K-1**−**K-8**. This material is available free of charge via the Internet at http://pubs.acs.org.

IC061737D